2024 IEEE/RSJ International Conference on Intelligent Robots and Systems (IROS)
October 14-18, 2024. Abu Dhabi, UAE

Decentralized Acceleration-Based Bird-Inspired Flocking

Luca Iacone[1], Erwin Lejeune[1], Tiziano Manoni[1,3], Sabato Manfredi[2], and Dario Albani[1]

Abstract— **In the following, we analyze and discuss the implementation of a novel approach for distributed flocking behavior applied to a group of Uncrewed Aerial Vehicle (UAV)s, also referred to as drones. Inspired by natural flocking phenomena observed in birds, which demonstrate coordinated movement in response to internal and external stimuli, we tackle the problem of robust and dynamic aerial motion for robots and design a control law based on a novel physical model. In contrast to previous works that rely on velocity or position-based references, this approach leverages an acceleration-based law to describe the collective dynamics of many interacting particles. As observed in the following, a third-order control possesses several advantages compared to first or second-order control, such as smoother transitions, better force balancing, and more responsive and dynamic behaviors. These advantages are thoroughly analyzed in the following, thanks to physics-based realistic simulations and field experiments with medium-sized UAVs in an unstructured outdoor environment.**

I. INTRODUCTION

Flocking and group motion behaviors are not new and, from the days of the rise of swarm robotics until today, have been extensively investigated. Nonetheless, many challenges remain unresolved, and with the advancement of technology and the increasing presence of robots in everyday life, flocking is still relevant. This is of particular importance in the field of UAVs. UAVs possess the capability to navigate infrastructure-less spaces, presenting a significant advantage in various applications. However, as the number of drones increases, the feasibility of maintaining effective communication among them diminishes, challenging the viability of a centralized control system. This limitation motivates the need for distributed approaches in various research fields such as swarm robotics, which is known for its intrinsic design robustness, reactivity, and the ability to dynamically reconfigure. From an operator's point of view, whether in agriculture, search and rescue, or defense, this poses a great benefit by enabling an operator to issue simple high-level commands, facilitating the emergence of collective behaviors without the necessity for individual drone control. This approach significantly reduces cognitive load on operators, enhancing operational efficiency and effectiveness in complex environments, even for basic behaviors such as motion.

Studies on group motion are numerous and range from classical swarm robotics approaches, such as those relying on virtual forces [1], [2], [3], to others on formation control used to deploy multi-agent systems into desired formation profiles [4], [5], [6], and learning-based approaches [7], [8]—just to cite a few. We purposely leave out the analysis of less classical, learning-based approaches for methodological reasons, and due to two main drawbacks: computational load and training time. Our main focus, which we believe matches those analyzed in the next section, is to design a reliable, robust, adaptable, and low computational load algorithm for group motion—not formation. To this end, we draw inspiration from recent research by Jung et al. [9], presenting a novel physical model for bird-flocking. The model extends the classical Cucker-Smale [1] flocking model and introduces individual reactions to neighboring changes of acceleration, allowing the birds (robots) to react to perturbations coming from the environment. This is, to the best of our knowledge, the first time an acceleration model for flocking has successfully moved from theory to practice in the field and is applied to a group of UAVs. The following sections delve into the implementation of the proposed model, its applicability to robotic platforms, and its deployment in the field, demonstrating its practical benefits and pioneering contributions to UAV flocking dynamics.

II. STATE OF THE ART

Since the seminal work by Reynolds [10], flocking and group motion have garnered increasing interest in the scientific communities, leading to the formulation of several approaches based on artificial intelligence, robotics, and consensus frameworks (see, for example, [8], [11], [12], [13] and references therein). Three heuristics are proposed that lay the foundation for future works such as [14]: Cohesion, where agents in the swarm are attracted to the average position of their respective neighbors; Separation, where robots are repelled from neighboring robots; and Alignment, where each agent converges to the average velocity of its neighbors. In a survey, Logan and Malikopoulos [15] analyze the recent state of the art for the decentralized aggregate motion of individuals—a.k.a. flocking. The authors propose a division of the state-of-the-art from an engineering perspective and identify two subsets: line flocking and cluster flocking. The former aggregates all those works where the objective is to minimize the energy consumption of the entire swarm, similarly to geese in nature. Cluster flocking encompasses those works—as the one here presented—where the designer aims to optimize a system-level cost function to control the policy of the individual in favor of behaviors at the swarm level. More recently, Kumar et al. [16] propose a different perspective than [15] by partitioning the aggregate

[1]Luca Iacone, Erwin Lejeune, Tiziano Manoni and Dario Albani are with the Autonomous Robotics Research Center, Technology Innovation Institute, Abu Dhabi, UAE {name.surname}@tii.ae

[2]Sabato Manfredi is with the Department Electrical Engineering and Information Technology, Federico II University, Naples, Italy smanfred@unina.it

[3]Tiziano Manoni is with the Department of Computer Science, Vrije Universiteit, Amsterdam, The Netherlands t.manoni@vu.nl

motion behaviors into flocking and swarming. In flocking, the agents primarily coordinate their direction of motion, while in swarming, they congregate in space to organize their spatial positions. From this alternative viewpoint, the approach proposed in this manuscript can be identified as flocking. Indeed, as previously introduced, we draw inspiration from the physical model proposed by Jung et al. in [9] that analyzes the behavior of birds flying in a flock by describing the control policy for a single bird. Thanks to this, birds constantly adjust their behaviors according to their neighbors' states, synchronizing dynamically, without losing coherence but still being reactive to external perturbations. The model extends the deterministic Cucker–Smale model [1] by including individual reactions to neighbors' acceleration, where the reactions are weighted according to the local state of polarity. More classical models such as Vicsek (discrete-time) [17], Cucker–Smale (continuous-time) [1], and more recently [18] still focus on the emergence of velocity synchronization, assuming the absence of sudden changes in speed. The main difference between these last models and the one we propose here is the level at which the control inputs are handled. Indeed, while [17], [1], [18] generate velocity control requests, we rely on higher-order inputs—i.e., acceleration—to ensure smoother control and dynamic adaptation to disturbances. Works such as those by Ferrante et al. [19], [20] seek to maintain specific positions during motion by locking in place the members of the swarm with controllers that seek the local minima of surrounding forces. These works have been designed with ground non-holonomic robots in mind, and only in [21] do we see the original control applied in the air. An impressive work that sparked considerable interest in the community is [22]. The approach relies on three main components: short-range potential repulsion, middle-range velocity alignment, and global position constraints for flocking and formation flights. The global position constraints are used to maintain the flock compact and achieve coherent motion and formation otherwise not achievable under the same conditions. Half-spring short-range potential repulsion is then used within the position boundaries to ensure separation and thus avoid collisions. Lastly, velocity alignment with viscous friction is used to dampen single agents' velocities in favor of synchronized collective motion. Other recent work, as by Albani et al. [3] and Manoni et al. [2], focuses on field applications and attempts to guide the swarm across a generic set of waypoints. The introduction of targets and positions through which the swarm must navigate poses challenges that are usually not investigated in classical flocking analysis or nature-focused work. Among these challenges is the trade-off between target forces and swarm forces. In [3], the decentralized flocking approach proposed builds over classical potential field models and is proven to work well at lower speeds in real-world environments. Here, each robot in the swarm relies on limited information and can only perceive its local neighbors through limited communication of noisy position information. The work from Manoni et al. builds on top of this [2] by introducing a Gaussian kernel to regulate the importance of each element in the swarm scheme and dynamically balance the target and swarm forces. UAVs in the swarm are then able to follow complex waypoints across space up to a speed of $8m/s$ after which the swarm started to show separation. To the best of our knowledge, all the works here analyzed are velocity-based, and no third-order control scheme has been applied to real robots outside the lab boundaries until now.

III. A THIRD-ORDER FLOCKING LAW

Before diving into the specifics, it's important to note that this is the first time an approach designed to control drone swarms at the acceleration level has been successfully implemented outside of a lab setting. The research by [23] shows how using acceleration feedback can significantly improve balance by compensating for reflex delays. This is particularly relevant to our work, where each drone calculates its movement based on noisy and delay-affected measurements, highlighting the foundation of our approach. It suggests that controlling a system through acceleration could offer a better way to handle the dynamic disturbances and measurement inaccuracies commonly found in real-world scenarios. Building on this principle, our proposed flocking algorithm is a third-order control law inspired by the innovative findings in [9], resulting in the final formulation of a bird-inspired acceleration controller for way-point navigation. It is comprised of four core components describing the dynamics of the flock: (i) neighbors attraction and repulsion control, (ii) target proximal control, (iii) velocity consensus, and (iv) acceleration synchronization. The proposed law combines all the above terms:

$$\mathbf{u}_i = \mathbf{v}_i^{neigh} + \mathbf{t}_i^{prox} + \mathbf{v}_i^{cons} + \mathbf{a}_i^{synch} \tag{1}$$

where u_i represents the target acceleration applied to each agent, i is the index of the $i-th$ agent in the swarm, and each term respectively identifies the four core vectorial components of the approach.

In the following, we rely on the following mathematical notations which allows us to concisely describe our acceleration-based model. All the individual states of the robot i are expressed in the same reference frame which is shared among all the units in the swarm: $\mathbf{p}_i = [p_i^x, p_i^y]'$ is the individual planar position; $\mathbf{v}_i = [v_i^x, v_i^y]'$ the instantaneous velocity; $\mathbf{a}_i = [a_i^x, a_i^y]'$ the instantaneous acceleration. Similarly, each $i-th$ individual in the swarm collects and stores all the available information about its neighbours: $\mathbf{p}_j \forall j \in N$ is the collection of all the positions of the N neighbouring agents with $i \notin N$; $\mathbf{v}_j \forall j \in N$ represents the vector collection of the velocities; $\mathbf{a}_j \forall j \in N$ is the collection of the accelerations.

A. Neighbors Attraction and Repulsion control

The first term in equation (1) is the neighbor's attraction and repulsion control regulating the interaction between the agents. It is a function of the agents' positions, and more

specifically only of the ones with whom each platform is able to communicate:

$$\mathbf{v}_i^{neigh} = \sum_{j \in N} \frac{C_r}{l_r} e^{-\frac{|\mathbf{d}_{ij}|}{l_r}} \frac{|\mathbf{d}_{ij}|}{\mathbf{d}_{ij}} - C_a |\mathbf{d}_{ij}| \mathbf{d}_{ij} \tag{2}$$

where $\mathbf{d}_{ij} = \mathbf{p}_i - \mathbf{p}_j$ represents the vector distance between the focal agent i and a neighbor j within range. The attraction term in equation (2) is then regulated by the sum of an attractive term weighted by the constant C_a. On the end, the repulsive term is governed by an exponential function tuned by the constant C_r scaled by l_r which determines the distance at which repulsion is triggered. Tuning for these parameters (and other parameters in the following) have been initially proposed in [9] and have then been empirically fine-tuned to achieve and keep an inter-agent distance of 15 meters during the flocking, all the parameters are reported in table II inside the appendix section.

B. Target Proximal Control

The target proximal control is responsible for steering the swarm through a predefined set of way-points expressed as global positions in the common reference frame and not being a function of the time. The target proximal control is a function of the velocity of each agent and the position of the swarm center of mass:

$$\mathbf{t}_i^{control} = \alpha(\mathbf{v}_R - \mathbf{v}_i)|\mathbf{v}_i| \tag{3}$$

where $\mathbf{v}_R = |A| \tanh(\mathbf{p}_c - \mathbf{p}_t)$, $\mathbf{p_c}$ is the vector position of the center of mass, and $\mathbf{p_t}$ the position of the target way-point. This approach enables precise control over the swarm's motion towards a desired target on the plane. It involves dynamically generating velocity references, v_R, that direct the swarm toward the next way-point. The magnitude of these velocity references is adjusted using the $tanh$ function, which takes the distance between the target and the swarm's center of mass as arguments. In other words, the target action is stronger the further the swarm is from the target enabling a smooth deceleration while approaching the destination. The term $|A|$ specifies the maximum amplitude of the velocity vector, which is then adjusted dynamically. This consideration is crucial for applications involving real robots, where maintaining system stability is crucial. Abrupt changes in acceleration or deceleration can lead to destabilization of the individual, potentially causing the UAV to enter oscillatory states. Moreover, in scenarios where strong external disturbances occur, if these are not adequately countered by tailored disturbance observer mechanisms, setting the reference velocity too low may hinder the swarm's ability to reach the desired waypoint.

C. Velocities Consensus

Utilizing the Cucker-Smale alignment rule, each agent adjusts its heading to align with the average direction of the swarm. This is achieved by calculating a weighted average of the orientations of all other agents within the swarm. Specifically, the contribution of each agent towards achieving consensus is determined by its interactions with the velocities of other platforms in the swarm. The velocity consensus contribution is governed as:

$$\mathbf{v}_i^{cons} = \sum_{j \in N} J_{ij}(\mathbf{v}_j - \mathbf{v}_i) \tag{4}$$

where J_{ij} is the interaction matrix used to compute the weighted average and measure the influence of all the neighboring agents $j \in N$ with respect to the focal agent i. This variable influence monotonically decays with the distance as $J_{ij} = K_v g(d_{ij})$, where $g(y) = \frac{1}{(1+y^2)^2}$; and K_v is the interaction strength for velocity.

D. Acceleration Synchronization

The last term introduced in our flocking equation is the main responsible for the increase of the reactivity of the swarm. It is defined according to the following:

$$\mathbf{a}_i^{sync} = \sum_{j \in N} I_{ij} \mathbf{a}_j \tag{5}$$

Equation (5) dynamics are similar to those in equation (4). Each agent is influenced by the acceleration of its neighbors, with the acceleration being weighted by a similar logic. I_{ij} is the interaction matrix for the acceleration synchronization term, it monotonically decays with the distance d_{ij} as $I_{ij} = K_a g(d_{ij})$, where $g(y) = \frac{1}{(1+y^2)^2}$; and K_a is the interaction strength for acceleration.

IV. RESULTS

To evaluate the merits and the limitations of the proposed flocking law on UAVs we present the results of extensive tests performed in simulation and in the desert of Abu Dhabi. We focus the analysis on two complex trajectories with different swarm sizes. Particularly, simulated and real experiments, see: (i) A swarm of 6 drones following a square trajectory of 250 meters side; (ii) A swarm of 9 drones following an 8-shaped Lissajous curve consisting of 16 consecutive way-points to reproduce the desired final shape.

For the tests in simulation, we rely on Ignition Gazebo using the DART physics engine due to its ability to mimic real-life physics and the possibility of including sensor noise but without the presence of wind. Each unit in the simulated swarm relies on its own instance of the same control stack built on top of the PX4 SITL used to convert the computed body rate and thrust commands to PWM for the rotors. Body rate and trust are produced by a low-level geometric tracking controller running at 100 Hz [24], which takes the target acceleration as its input.

For outdoor experiments, we rely on the same low-level control stack that is however deployed on custom quad-rotors built by the team at the Technology Innovation Institute (TII). These are mid-size quad-copters equipped with the flight controller Pixhawk 6X, standard GPS—no RTK—for navigation, and onboard computers for decentralized processing of the information. Drones are able to communicate through 5.8GHz radios with communication not being ensured at

Fig. 1: Aerial viewpoint from one drone during the experiments.

all times. The real tests also threw in challenges like non-constant wind speeds of $7m/s$ and gusts hitting $11m/s$.

To fairly evaluate the capabilities of our implementation, we compare it against the work of Manoni et al. [2]. It is crucial to note that these comparisons have been carried on only in simulation over a total of 10 runs for each of the proposed approaches and trajectories.

Results follow the analysis of the metrics introduced in [2]: **CAP**, Cluster APproach velocity (CAP); And **COR**, CORrelated unit velocity (COR). The CAP expresses the ratio of the average velocity of the cluster while flocking in relation to the maximum allowed velocity v_{max} of the individual. This results in values ranging between 1, when the average velocity for the cluster is equal to Vmax, and 0, no motion.

$$CAP = \frac{\sum_{i \in C} |\mathbf{v}_i| cos(\theta_c)}{|C||v_{max}|} \tag{6}$$

In the equation, the term v_i represents the velocity vector of the $i-th$ agent belonging to the cluster C. Each velocity is then scaled according to the angle between the velocity direction and the velocity of the center of mass of the cluster.

The COR is then used to analyze the relationship between the single robot velocity v_i and the cluster center of mass velocity v_c. In contrast with the CAP, which refers to the performance of the whole cluster, the COR is used to validate each agent velocity and is expressed as:

$$COR = \frac{|\mathbf{v}_i| cos(\theta_c)}{|\mathbf{v}_c|} \tag{7}$$

This metric is useful to separate the cluster motion, expressed with the CAP from possible oscillations of the single robot induced by the flocking controller.

A. Real Robot Experiment

We start the analysis with real robot experiments. We analyze the results of the algorithm on our target platform over 2 runs for each of the proposed trajectories reporting COR, CAP, average ground speed, and the planar trajectories of each unit over time. Results for the Lissajous-trajectory are reported in Figure 2.

From analysis of the Lissajous trajectory, as detailed in Figure 2 we can appreciate the swarm adaptability while performing the complex trajectory. The units are able to maintain continuous coherent motion for approximately five minutes and cover a noteworthy distance of almost 2 kilometers. Of particular interest is the peak velocity, which reaches up to 8 meters per second as requested. The implementation of velocity term in equation (1) here plays a critical role, especially as the swarm navigates towards way-points. The use of the $\tanh$ function forces the control law to tailor the reduction and increase of the speed during the crossing of the way-points ensuring stability during turns and sharp directional changes. Moreover, while on linear segments of the trajectory, the velocity is pushed and kept at the desired speed of $8m/s$.

The performance in terms of CAP (6) and COR (7), as depicted in Figure 2, is notable—more on this in the simulation comparisons. The CAP metric, illustrated by a solid blue line in Figure 2, fluctuates between 0.75 and the optimal value of 1 throughout the experiment even in presence of very high wind disturbance of up to $11m/s$ During the straight sections, the optimal CAP values are achieved with consistency showing the good balancing of the control law. Similarly to the speed behavior, during turns, way-point crossing, and sharp changes in the direction of motion adjustments automatically take place as observed by a slight diminution of the CAP metric. The COR metric exhibits oscillations around the ideal value of 1, again with the best performance observed during the linear stretches. The variability of the COR metric is pronounced at the trajectory's extremities, coinciding with the lowest velocities and indicating how the algorithm acts in ensuring a good formation alignment.

To further validate the robustness and reliability of our acceleration-based flocking, we also present field experiments over a squared-shaped trajectory. These experiments have been performed with a smaller swarm to validate the algorithm's scalability. The size of the swarm during these experiments is set to be 6 UAVs. Results are shown in Figure 3, showcasing both the trajectory, the velocities, and the two studied metrics. The squared trajectory, due to its intrinsic simplicity and to a decrease in the number of way-points, allows the swarm to better align and maintain the reference velocity of $8m/s$. Moreover, thanks to a reduced number of turns and requested target positions, the swarm

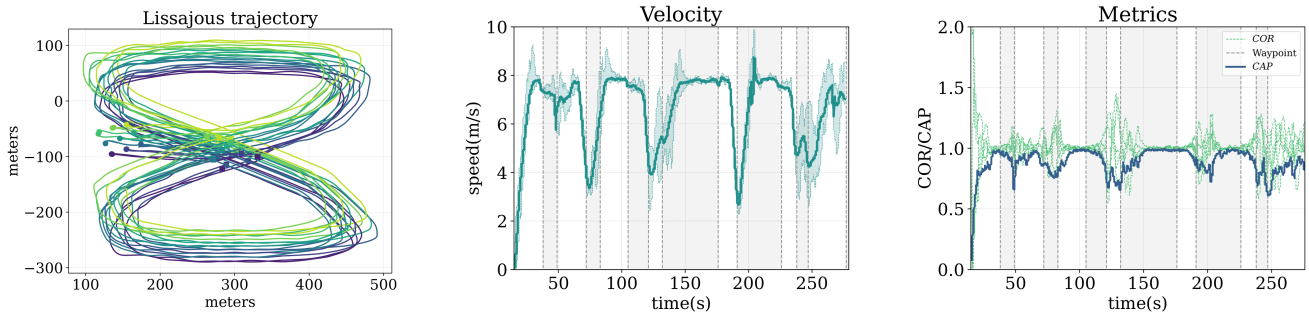

Fig. 2: Results for the Lissajous-shaped trajectory field experiments. Left-to-right: (i) Trajectories over 2 runs of the individuals in the swarm. A circle represents the starting point, a square represents the end point of the trajectory; (ii) Velocity the swarms center of mass averaged over 2 runs; (iii) CAP, solid blue line, and COR, dashed green line, averaged over 2 runs. Higher CAP y-values yield better performances. Close to 1 y-values show better COR performance.

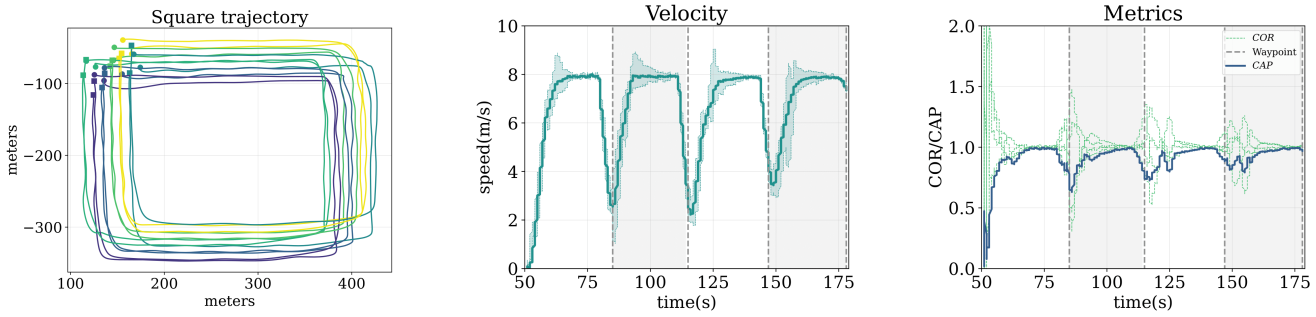

Fig. 3: Results for the Square-shaped trajectory field experiments. Left-to-right: (i) Trajectories over 2 runs of the individuals in the swarm. A circle represents the starting point, a square represents the end point of the trajectory; (ii) Velocity the swarms center of mass averaged over 2 runs; (iii) CAP, solid blue line, and COR, dashed green line, averaged over 2 runs. Higher CAP y-values yield better performances. Close to 1 y-values show better COR performance.

has more time to adapt to the external disturbances. This can be appreciated by analysis of the velocity profiles and the metrics in the figure. Finally, results are unaffected by the agents' starting positions. This is demonstrated by repeated experiments with different initial positions (Figure 3, left).

B. Simulation Analysis

To further validate our proposed approach, we extended our analysis to include simulations in addition to the real drone experiments. Simulations have been conducted using the Ignition Gazebo, a highly realistic environment that emulates real-world physics and sensor noise. The model of the drones used in simulation resembles the one used for the real-world experiments, the low-level controller and the entire control stack are maintained as per the real experiments.

Simulated experiments see the same setup as the field experiments but with a higher number of runs for each trajectory and with a direct comparison between the acceleration-based control law and the work from Manoni et al. [2]. The latter is chosen as a benchmark since it proposes and introduces the same flocking behavior through multiple consecutive way-points; a feature that is not commonly found in other flocking approaches, where the agents are left focusing on the coordination rather than navigation through way-points. Presented results are obtained by averaging over 10 different runs and by initializing the agents, at the start of each run, in positions similar to those reported during the field experiments. The aim, during this process, has been to closely replicate the conditions of the real-world tests.

The results, covering both the Lissajous and square trajectories, are illustrated in Figure 4. The first column in the figure shows the trajectories for both the Lissajous and Square shape, by alternating the results (each row) respectively for the acceleration-based control law and Manoni et al. Each figure shows 10 overlapping runs with a bold red-dashed line indicating the placement of the original way-points. The remaining columns show the respective values for the velocity and the COR and CAP metrics, again each row alternating between the here presented approach and its counterpart.

By visual analysis of the figures, we immediately note that both approaches are able to perform the requested trajectories without any collisions and ensure cohesiveness and accuracy. Accuracy that is better ensured by the newly presented approach that, across the multiple runs, shows consistency and repeatability almost never deviating from the original path from one run to the other.

The difference in the speed of the center of mass and its variance over the different runs is notable (shadowed section in the plot). While the approach by Manoni et al. is able to

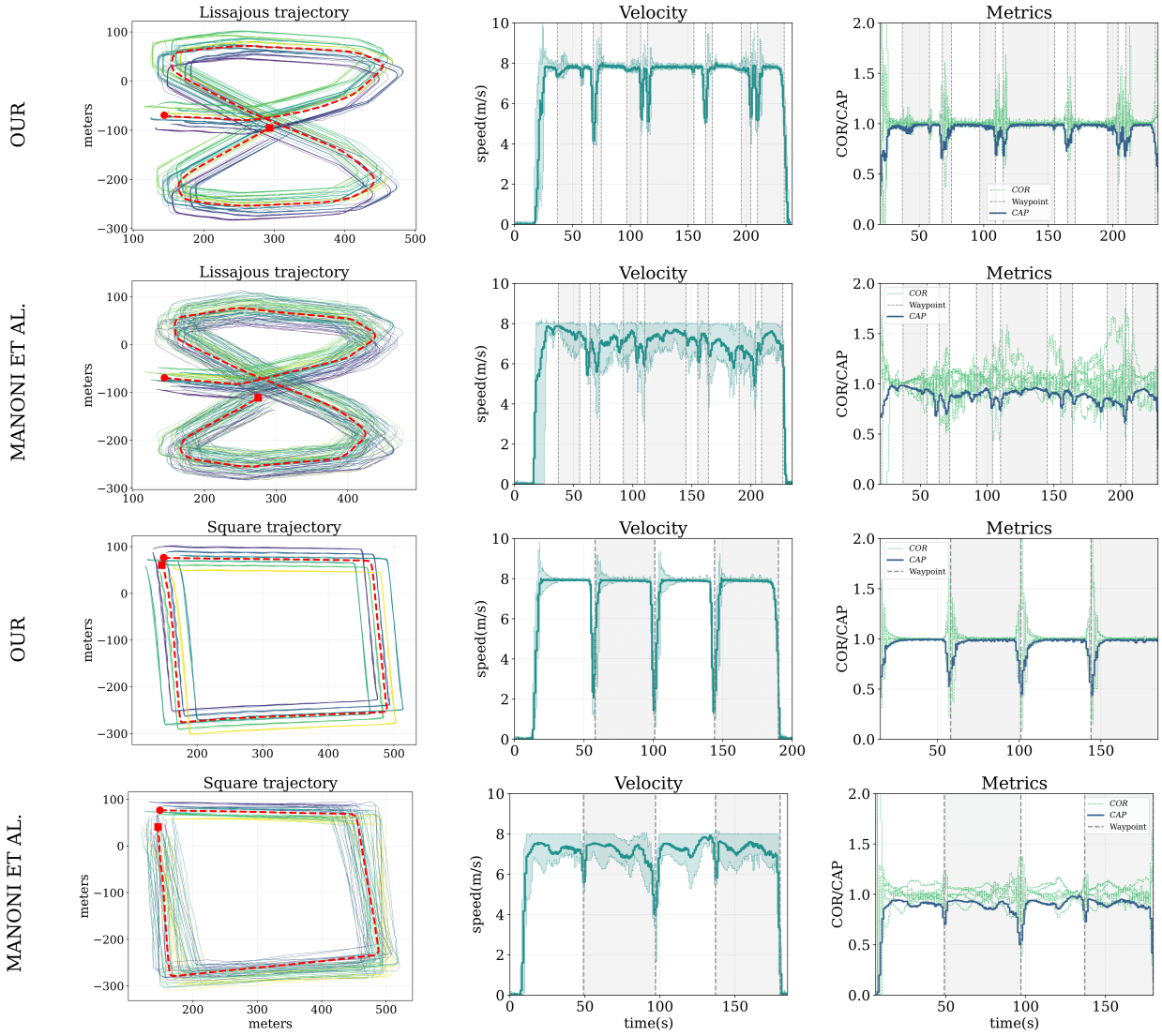

Fig. 4: Comparison of the two approaches in simulation. Left-to-right: The achieved trajectories across 10 runs. Red dashed line indicates the original position of the way-points; Average velocity analysis, the shadowed region indicates the variance computed across all the runs; CAP and COR metrics, again averaged across the different runs. Top-Down: Each row alternates the results respectively for the acceleration-based control law here presented, and the approach by Manoni et al.

achieve a higher average speed throughout the whole process, one can clearly see that the speed is not consistent across the different runs and that the variance is higher. Not only, while the acceleration control law is able to achieve and stabilize across the maximum request velocity v_{max}, the same is not true for the competing approach.

C. Benchmark Comparisons

The analysis of the two metrics, COR and CAP, further validates the above findings. In the case of the approach proposed in [2], the CAP metric never reaches the optimal value, for both trajectories and swarm size, indicating a non-optimal approach of the swarm toward the waypoint. Similar reasoning applies to the COR metric that shows a high variance in the correlation of the velocities of the individuals in the swarm. On the other end, the newly proposed approach shows superior performances in terms of stability and excels in consistency. Notably, the simulation results are similar to those observed during the field experiments, highlighting the adaptability of the approach in the presence of strong external disturbances such as wind, unstable communication, and higher positioning noise.

This comparison is particularly important and underscores the enhanced stability and uniformity during the flocking that is ensured by a higher-level control strategy—i.e., acceleration vs velocity. Moreover, unlike the strategy presented by Manoni et al., which lacks a velocity synchronization feature, our approach benefits from such advanced control mechanisms, leading to superior performance metrics and more consistent velocity profiles. However, it is worth noting

that the competing approach does maintain steadier velocities across the different trajectories, avoiding excessive slow-downs when navigating through waypoints. An aggregate version of the CAP metric has been reported in table I to confirm the findings, proposing a simpler comparison between the algorithms.

TABLE I: Aggregate CAP metric from simulation experiments.

Algorithm	Shape	Value
Ours	Square	0.831
Manoni *et al.*	Square	0.830
Ours	Lissajous	0.867
Manoni *et al.*	Lissajous	0.782

V. CONCLUSIONS

In this work, we presented a novel controller for a swarm of unmanned aerial vehicles that, to the best of our knowledge, is the first to attempt to apply a third-order control law for flocking in realistic settings. The approach has been shown to be efficient, scalable, and able to handle complex trajectory even in presence of high external perturbations. We also compared the system against a recent model proposed by [2], showing its superiority in such conditions. Future work, will focus on increasing the speed at which the flock navigates the environment, and most importantly on testing the reactivity of the model, ensured by the control in acceleration, in case of obstacles, drone failures, and malicious agents.

VI. APPENDIX

To ensure that the proposed approach is reproducible and to foster further developments and research, we report the parameters used during the experiments along with a brief explanation.

TABLE II: Parameters and their meanings with values used in the study.

Parameter	Meaning	Value Used
C_r	Repulsion Constant Weight	70
l_r	Repulsion Triggering Factor	7
C_a	Attraction Constant Weight	0.00054
α	Target Control Gain	0.5
K_v	Velocity Interaction Strength	2000
K_a	Acceleration Interaction Strength	100

The parameters were initially scaled in magnitude during a first analysis approach to the model's equations conducted in MATLAB with the starting model [9], later the values were empirically fine-tuned in simulation and refined during field experiments, achieving the final values reported in the table II.

REFERENCES

[1] Felipe Cucker and Steve Smale. Emergent behavior in flocks. *IEEE Transactions on automatic control*, 52(5):852–862, 2007.

[2] Tiziano Manoni, Dario Albani, Jiri Horyna, Pavel Petracek, Martin Saska, and Eliseo Ferrante. Adaptive arbitration of aerial swarm interactions through a gaussian kernel for coherent group motion. *Frontiers in Robotics and AI*, 9:1006786, 2022.

[3] Dario Albani, Tiziano Manoni, Martin Saska, and Eliseo Ferrante. Distributed three dimensional flocking of autonomous drones. In *2022 International Conference on Robotics and Automation (ICRA)*, pages 6904–6911. IEEE, 2022.

[4] Jinwen Hu, Houxin Zhang, Lu Liu, Xiaoping Zhu, Chunhui Zhao, and Quan Pan. Convergent multiagent formation control with collision avoidance. *IEEE Transactions on Robotics*, 36(6):1805–1818, 2020.

[5] Junyan Hu, Parijat Bhowmick, Inmo Jang, Farshad Arvin, and Alexander Lanzon. A decentralized cluster formation containment framework for multirobot systems. *IEEE Transactions on Robotics*, 37(6):1936–1955, 2021.

[6] Gerhard Freudenthaler and Thomas Meurer. Pde-based multi-agent formation control using flatness and backstepping: Analysis, design and robot experiments. *Automatica*, 115:108897, 2020.

[7] Shao-Ming Hung and Sidney N. Givigi. A q-learning approach to flocking with uavs in a stochastic environment. *IEEE Transactions on Cybernetics*, 47(1):186–197, 2017.

[8] Chao Yan, Chang Wang, Xiaojia Xiang, Zhen Lan, and Yuna Jiang. Deep reinforcement learning of collision-free flocking policies for multiple fixed-wing uavs using local situation maps. *IEEE Transactions on Industrial Informatics*, 18(2):1260–1270, 2022.

[9] Narina Jung, Byung Mook Weon, and Pilwon Kim. Effects of adaptive acceleration response of birds on collective behaviors. *Journal of Physics: Complexity*, 3(1):015014, 2022.

[10] Craig W Reynolds. Flocks, herds and schools: A distributed behavioral model. In *Proceedings of the 14th annual conference on Computer graphics and interactive techniques*, pages 25–34, 1987.

[11] Logan E. Beaver and Andreas A. Malikopoulos. An overview on optimal flocking. *Annual Reviews in Control*, 51:88–99, 2021.

[12] Sabato Manfredi and David Angeli. Necessary and sufficient conditions for consensus in nonlinear monotone networks with unilateral interactions. *Automatica*, 77:51 – 60, 2017.

[13] Sabato Manfredi and Edmondo Di Tucci. Decentralized control algorithm for fast monitoring and efficient energy consumption in energy harvesting wireless sensor networks. *IEEE Transactions on Industrial Informatics*, 13(4):1513 – 1520, 2017.

[14] William Crowther. Rule-based guidance for flight vehicle flocking. volume 218, pages 111–124, 04 2004.

[15] Logan E Beaver and Andreas A Malikopoulos. An overview on optimal flocking. *Annual Reviews in Control*, 51:88–99, 2021.

[16] Gourab Kumar Sar and Dibakar Ghosh. Flocking and swarming in a multi-agent dynamical system, 2023.

[17] Tamás Vicsek, András Czirók, Eshel Ben-Jacob, Inon Cohen, and Ofer Shochet. Novel type of phase transition in a system of self-driven particles. *Phys. Rev. Lett.*, 75:1226–1229, Aug 1995.

[18] Martial Agueh, Reinhard Illner, and Ashlin Richardson. Analysis and simulations of a refined flocking and swarming model of cucker-smale type. *Kinetic and Related Models*, 4(1):1–16, 2011.

[19] Eliseo Ferrante, Ali Emre Turgut, Cristián Huepe, Alessandro Stranieri, Carlo Pinciroli, and Marco Dorigo. Self-organized flocking with a mobile robot swarm: a novel motion control method. *Adaptive Behavior*, 20(6):460–477, 2012.

[20] Eliseo Ferrante, Ali Turgut, Alessandro Stranieri, Carlo Pinciroli, Mauro Birattari, and Marco Dorigo. A self-adaptive communication strategy for flocking in stationary and non-stationary environments. *Submitted to Natural Computing, moderate revisions*, 13, 06 2013.

[21] Thulio Amorim, Tiago Nascimento, Pavel Petracek, Giulia de Masi, Eliseo Ferrante, and Martin Saska. Self-organized uav flocking based on proximal control. In *2021 International Conference on Unmanned Aircraft Systems (ICUAS)*, pages 1374–1382, 2021.

[22] Gábor Vásárhelyi, Csaba Virágh, Gergő Somorjai, Tamás Nepusz, Agoston E Eiben, and Tamás Vicsek. Optimized flocking of autonomous drones in confined environments. *Science Robotics*, 3(20):eaat3536, 2018.

[23] Tamás Insperger, John Milton, and Gábor Stépán. Acceleration feedback improves balancing against reflex delay. *Journal of the Royal Society Interface*, 10(79):20120763, 2013.

[24] Taeyoung Lee, Melvin Leok, and N. Harris McClamroch. Geometric tracking control of a quadrotor uav on se(3). In *49th IEEE Conference on Decision and Control (CDC)*, pages 5420–5425, 2010.